Structure–Activity Correlations of Melanotropin Peptides in Model Lipids by Tryptophan Fluorescence Studies

Amando S. Ito,‡ Ana M. de L. Castrucci,§ Victor J. Hruby,‖ Mac E. Hadley,⊥ Donald T. Krajcarski,# and Arthur G. Szabo*,#

Instituto de Fisica da Universidade de Sao Paulo, C. Postal 20516, 01498 Sao Paulo, Brazil, Instituto de Biociências da Universidade de Sao Paulo, C. Postal 11176, 05499 Sao Paulo, Brazil, Departments of Chemistry and Anatomy, University of Arizona, Tucson, Arizona, 85721, and Institute for Biological Sciences, National Research Council, Ottawa, Canada K1A OR6

Received February 8, 1993; Revised Manuscript Received August 13, 1993®

ABSTRACT: Steady-state and time-resolved fluorescence spectroscopy were employed in the study of the structure and interactions of α-MSH (α-melanocyte-stimulating hormone) and its analogs, [Nle^4,D-Phe^7]-α-MSH (MSH-I) and Ac-[Nle^4,Asp^5,D-Phe^7,Lys^{10}]-α-MSH(4–10)-NH$_2$ (MSH-II). In aqueous buffer, the fluorescence parameters of the single tryptophan of α-MSH and MSH-I were similar and did not allow any distinction between these molecules. On the other hand, the tryptophan fluorescence of MSH-II was notably different, reflecting its cyclic lactam turn structure. In the presence of acidic lipid vesicles, the fluorescence properties of the peptides were different, indicating structural changes on incorporation of the peptide into the liquid-crystalline phase of the lipid. No evidence of interaction was observed in the presence of the neutral lipid dimyristoylphosphatidylcholine (DMPC). The association constants for lipid–peptide interactions were compared for binding isotherms which either neglected or accounted for electrostatic effects through Gouy–Chapman potential functions. The relative order of association constants in either treatment was MSH-II > MSH-I > α-MSH. These results parallel the reported biological activities that show increased potencies and prolongation of response for the analogs, MSH-II and MSH-I, as compared to the native hormone, α-MSH. Time-resolved fluorescence results showed that the fluorescence decay of melanotropins is best described by triple-exponential kinetics. In the lipid–peptide complex, there was a change in the relative concentrations of the components, with the intermediate-lifetime component predominating compared to those in solution. The results are consistent with a model where the peptides are initially attracted electrostatically to the vesicle surface and are then incorporated into the lipid phase, due to hydrophobic forces with accompanying conformational changes, to form a compact reversed turn structure.

Melanotropins are peptide hormones known to activate pigment cells. In most vertebrates, α-MSH[1] (α-melanocyte-stimulating hormone) is the physiologically relevant hormone regulating skin pigmentation. α-MSH is a tridecapeptide whose amino acid sequence is Ac-Ser-Tyr-Ser-Met-Glu-His-Phe-Arg-Trp-Gly-Lys-Pro-Val-NH$_2$. It is derived from the precursor protein, pro-opiomelanocortin, and is secreted from the *pars intermedia* of the pituitary gland (Sawyer et al., 1980; Al-Obeidi et al., 1989; Castrucci et al., 1990). Clinically, the melanotropic peptides may be used for pigmentary disorders and the detection and eradication of melanoma cancer (Hruby et al., 1984; Hadley et al., 1985).

In skin bioassays, it was shown that the central 6–9 tetrapeptide, His-Phe-Arg-Trp, is the melanotropic minimal message sequence of α-MSH and is absolutely required for biological activity. The minimal effective sequence for equipotency to α-MSH in the frog skin bioassay is Ac-α-MSH(4–12)-NH$_2$ and that in the lizard skin bioassay is Ac-α-MSH(4–11)-NH$_2$. Substitution of Nle for Met^4 generally results in more potent derivatives. In addition, substitution of the D enantiomer of Phe^7 into the Nle^4-modified analog of α-MSH resulted in the analog [Nle^4,D-Phe^7]-α-MSH (hereafter referred to as MSH-I), which in the frog skin bioassay exhibits increased potency and prolonged activity as compared to the corresponding L-amino acid containing analog (Sawyer et al., 1980). Cyclic lactam analogs of α-MSH also have been designed and synthesized (Al-Obeid et al., 1989a). The peptide Ac-[Nle^4,Asp^5,D-Phe^7,Lys^{10}]-α-MSH(4–10)-NH$_2$ (hereafter referred to as MSH-II) is about 90 times more potent than α-MSH in the lizard skin bioassay and also exhibits residual activity when compared to the native molecule (Al-Obeidi et al., 1989b).

It has been suggested that α-MSH interaction with melanocyte membrane receptors activates adenylate cyclase, leading to increased intracellular levels of cyclic AMP (Hadley & Castrucci, 1988; Sawyer et al., 1988; Hruby et al., 1984). The mononucleotide, acting as a second messenger, triggers a cascade of phosphorylations, leading to de-repression of specific genes with an increase in the activity of tyrosinase, the enzyme responsible for the first set of reactions in melanin synthesis. The increasing activities of the synthetic analogs of α-MSH may reflect varying strengths of peptide–receptor interactions. However, according to the general model of Schwyzer, the lipid phase of the cell membrane may function as a catalyst for ligand–receptor interactions (Sargent & Schwyzer, 1986; Schwyzer, 1986). Investigation of the

* Author to whom correspondence should be addressed.
‡ Instituto de Fisica da Universidade de Sao Paulo.
§ Instituto de Biociências da Universidade de Sao Paulo.
‖ Department of Chemistry, University of Arizona.
⊥ Department of Anatomy, University of Arizona.
National Research Council.
® Abstract published in *Advance ACS Abstracts,* November 1, 1993.
[1] Abbreviations: α-MSH, α-melanocyte-stimulating hormone; MSH-I, [Nle^4,D-Phe^7]-α-MSH; MSH-II, [Nle^4,Asp^5,D-Phe^7,Lys^{10}]-α-MSH-(4–10)-NH$_2$; MML, monomyristoylphosphatidylcholine; DMPC, dimyristoylphosphatidylcholine; DMPG, dimyristoylphosphatidylglycerol; DMPS, dimyristoylphosphatidylserine; POPS, palmitoyloleylphosphatidylserine; DAS, decay-associated spectra; NATA, *N*-acetyltryptophanamide.

0006-2960/93/0432-12264$04.00/0 Published 1993 by the American Chemical Society

interactions between melanotropins and lipid vesicles, which serve as an *in vitro* model of biological membranes, may usefully clarify the role of the lipid phase in hormonal action.

Fluorescence spectroscopy has been widely used to study peptide–lipid interactions and the peptide structure and dynamics of such complexes when tryptophan is present in the peptides (Cavatorta et al., 1991; Willis & Szabo, 1992). α-MSH possesses a single tryptophan residue at position 9, which is essential for the biological activity of the hormone. We were interested in obtaining information on the properties of the peptides in aqueous solution and on the effect of their interaction with model membranes. Acidic lipids have a negative Gouy–Chapman potential, attracting any positively charged species present in the medium (Seelig & MacDonald, 1989; McLaughlin, 1977). As α-MSH and its analogs have a net positive charge, the electrostatic attraction should be taken into account in determining binding constants of the lipid–peptide interaction. Steady-state fluorescence measurements allow the estimation of these binding constants, as well as give insights into the environment of the peptide in the lipid complex. Time-resolved fluorescence spectroscopy can provide additional information about changes in the structure of the peptides and the concomitant change in conformational heterogeneity of the tryptophan residue upon binding of the peptide to lipids. Such fluorescence spectroscopic studies of α-MSH and its analogs, both in aqueous solution and in the presence of neutral and charged lipids, are reported herein.

MATERIALS AND METHODS

α-MSH was purchased from Sigma Chemical Co. (St. Louis, MO) and used without additional purification. Analogs of α-MSH, including Ac-α-MSH(7–10)-NH_2, MSH-I, and MSH-II, were synthesized and purified as described elsewhere (Hruby et al., 1987; Sawyer et al., 1980; Al-Obeidi et al., 1989). Melanotropins were used at concentrations of (1.0–2.5) × 10^{-5} M.

Lipids were obtained from Avanti Polar Lipids (Birmingham, AL) and used without further purification. Vesicles were prepared by the method of extrusion (Hope et al., 1985), resulting in 10 mM stock suspensions. The buffer used was either potassium phosphate or sodium cacodylate (0.01 M, pH 7.0). The lipids employed were monomyristoyllecithin (MML), dimyristoylphosphatidylcholine (DMPC), dimyristoylphosphatidylglycerol (DMPG), dimyristoylphosphatidylserine (DMPS), and palmitoyloleylphosphatidylserine (POPS).

Lipid titrations were performed by adding small amounts of the concentrated lipid vesicle suspensions to the hormone solutions and monitoring the fluorescence intensity changes of the peptide tryptophan fluorescence. From these titration curves, the concentration of bound peptide, $[P_b]$, could be estimated according to $[P_b] = [P_T](I - I_o)/(I_{max} - I_o)$, where I is the fluorescence intensity after the addition of an aliquot of lipid, I_o is the initial intensity of the peptide in the absence of lipid, and I_{max} is the plateau value of the fluorescence intensity reached after the addition of an excess of lipid. Scatchard plot analyses were performed using data from titration curves such as those shown in Figure 3, with the saturation value being that listed in Table II.

Absorption spectra were measured using a Varian DMS200 spectrophotometer. Steady-state fluorescence was measured with an SLM Aminco 8000C spectrofluorimeter. The excitation and emission bandpass values were 4 nm. All fluorescence spectra were corrected for the instrumental sensitivity variation with wavelength. Fluorescence quantum yields, ϕ_f, were determined using solutions with absorbancies of <0.1 at the excitation wavelength. NATA in pH 7 buffer, 20 °C, was used as a fluorescence quantum yield standard, taking the value of $\phi_f = 0.14$ (Szabo & Rayner, 1980). The steady-state fluorescence anisotropy was measured at 340 nm using Glan Taylor polarizers in a T-format configuration, with monochromators in each arm of the detection system. The G factor, $G = I_{HV}/I_{HH}$, was determined for each set of measurements. The values of the fluorescence anisotropy were the averages of three determinations. The temperature was controlled with a Neslab Endocal refrigerated circulating bath. Time-resolved fluorescence experiments were performed using an apparatus based on the time-correlated single photon counting method. The excitation source was a cavity-dumped dye laser synchronously pumped by a mode-locked argon laser (Spectra Physics) operating at 825 kHz, giving a pulse width of 10 ps. The 590-nm output of the dye laser was frequency-doubled with a KD*P crystal to give the sample excitation wavelength of 295 nm. Fluorescence emission was detected at right angles after passage through a Glan Taylor calcite polarizer oriented at 55° and a JY H10 monochromator with 4-nm bandpass on a Hamamatsu 1564U-01 microchannel plate photomultiplier. The FWHM of the instrument response function (IRF) was typically 60 ps. A single decay curve would usually contain a total of >1 000 000 counts in 1024 channels of a multichannel analyzer with a channel width of 20 ps. In all cases the signal from an appropriate blank was subtracted from the decay of the sample. Other details of the time-resolved method, instrumentation, and data analysis have been reported earlier (Hutnik & Szabo, 1989; Willis & Szabo, 1989). The adequacy of the exponential decay fitting was judged by established criteria for inspection of the plots of weighted residuals and by statistical parameters, such as reduced χ-square and serial variance ratio (MacKinnon et al., 1977).

Table I: Fluorescence Quantum Yields for Melanotropin Peptides in Aqueous Solution[a]

peptide	quantum yield 20 °C	30 °C	40 °C
α-MSH	0.100	0.083	0.078
MSH(7–10)	0.084	0.071	0.065
MSH-I	0.105	0.089	0.083
MSH-II	0.095	0.082	0.080

[a] The excitation wavelength was 295 nm. Solutions were in 0.01 M phosphate buffer (pH 7.0). ϕ_f values were obtained using NATA as standard with a quantum yield of 0.14. ϕ_f values in 30 and 40 °C columns were obtained relative to measurements of NATA made at 20 °C.

RESULTS AND DISCUSSION

Fluorescence in Aqueous Solutions. In aqueous solutions of the melanotropins, the tryptophan fluorescence is similar to that of NATA in aqueous solution. Fluorescence emission spectra of aqueous solutions of all melanotropins excited at 295 nm show an emission maximum at 350 nm. The ϕ_f's of the peptides at pH 7.0 and 20 °C are nearly equal, with values close to 0.10 (Table I), a value typical of tryptophan in peptides. The steady-state fluorescence anisotropies of these peptide solutions were close to zero.

Interaction with Lipids. Aliquots of lipids were added to the peptide solutions, and the fluorescence parameters were monitored. Experiments were performed at temperatures where the lipid system was in the liquid-crystalline phase (20 °C for POPS, 30 °C for DMPG, and 40 °C for DMPS). The fluorescence emission spectrum of the tryptophan of α-MSH when the peptide was in the complex with POPS vesicles at a lipid/peptide (L/P) ratio of 63:1 shifted to lower wavelength

Table II: Relative Increase of Fluorescence Intensities for Melanotropin Peptides in Complexes with Lipids[a]

	MSH	MSH(7–10)	MSH-I	MSH-II
MML	1.93	2.10	1.92	nd
	(90)	(140)	(120)	
POPS (20 °C)	1.30	nd	1.44	1.77
	(70)		(65)	(40)
DMPG (30 °C)	1.18	1.22	1.16	1.06
	(40)	(35)	(40)	(43)
DMPS (40 °C)	1.35	1.80	1.40	1.72
	(110)	(80)	(90)	(40)

[a] Numbers in parentheses are the saturating L/P ratios. A value of 1.0 was assigned to the fluorescence intensity in the absence of lipid. Peptide concentrations were in the range (1–2) × 10^{-5} M in 0.01 M phosphate buffer (pH 7.0). All values were corrected for dilution after lipid addition.

Table III: Fluorescence Spectral Maximum Shift to Lower Wavelength (in nm) and Fluorescence Anisotropy of Melanotropin Peptides in Complexes with Lipids[a]

	α-MSH	MSH(7–10)	MSH-I	MSH-II
		Spectral Shifts		
MML	9.0	10.0	6.5	nd
POPS (20 °C)	7.0	nd	9.0	13.0
DMPG (30 °C)	12.0	11.0	10.0	10.0
DMPS (40 °C)	9.0	13.0	7.0	13.0
		Anisotropy Values		
MML (20 °C)	0.088	0.063	0.087	nd
POPS (20 °C)	0.072	nd	0.085	0.093
DMPG (30 °C)	0.097	nd	nd	0.102
DMPS (40 °C)	0.090	0.050	0.079	0.110

[a] The peptide concentrations were as in Table II, and the L/P was above the plateau value.

(343 nm) and showed an increase in fluorescence intensity. Similar, but not identical, changes (Tables II and III) in fluorescence emission spectra were observed for α-MSH, MSH-I, and MSH-II in all of the acidic lipid vesicles studied. The change in spectral maximum position (Table III) is due to the entry of the tryptophan residue into a more hydrophobic environment, such as that found in a less solvent-exposed lipid interior.

When the tryptophan residue moves from an aqueous to a lipid phase, a blue shift of the fluorescence spectral maximum and an increase in fluorescence intensity (Table II) are often observed (Jain et al., 1985; Surewicz & Epand, 1984; Yamashita et al., 1989; Chung et al., 1992; McKnight et al., 1991). The extent of the increase in fluorescence intensity depends on the particular peptide and lipid vesicle. This implies that the nature of the interaction of the individual peptides with the lipids varies for each peptide. The increase in fluorescence intensity results from a reduction in the non-radiative deactivation processes that involve interactions with solvent. In the presence of micelles of MML and vesicles of DMPS, DMPG, and POPS, α-MSH and its analogs display similar, but not identical, fluorescence spectral behavior. The variation in fluorescence intensity and in spectral maximum shift with increasing L/P for MSH-II and POPS vesicles is shown in Figure 1. The complexes formed with MML micelles had spectral behavior similar to that of complexes with acidic lipids. In fact, in the micelles, the fluorescence intensity (Table II) increased by almost a factor of 100%. In the acidic lipid vesicles, the increase ranged from 30 to 80% in phosphatidylserine vesicles, but only changed by 6–22% in phosphatidylglycerol. The spectral maximum shifts (Table III) were comparable for all complexes, including those with micelles.

In the presence of DMPC vesicles, no change in fluorescence intensity nor in peak position was observed. In addition, no evidence of interaction was observed when the peptides were added to mixed lipid vesicles of DMPC/DMPS (80:20), with the exception of the small analog, Ac-α-MSH(7–10)-NH_2, which showed an increase of 20% in fluorescence intensity at lipid/peptide ratios greater than 70. Furthermore, the fluorescence anisotropy of the peptide/DMPC mixture was zero. These observations demonstrate conclusively that a net negative charge on the lipids was essential for the formation of a peptide–lipid vesicle complex, with the exception of Ac-α-MSH(7–10)-NH_2, which is an antagonist for α-MSH. The situation in the micelles must be that the lack of any organized structure of the micelle surface or interior allows the peptides to interact with the lipid interior through hydrophobic interactions.

Another parameter that reflected the interaction of the peptide with the lipid was the tryptophan fluorescence anisotropy. There was a significant increase (Table III) in this parameter in the presence of lipid vesicles. It might be expected that this value should have been even higher in the lipid–peptide complex, if the tryptophan residue were completely restricted in its flexibility in the lipid environment. If such were the case, then the fluorescence anisotropy should reflect the rotation of the vesicle particle, which would be quite slow in terms of the tryptophan fluorescence decay time. The data then suggest that the tryptophan residue has some local flexibility in the lipid–peptide complex.

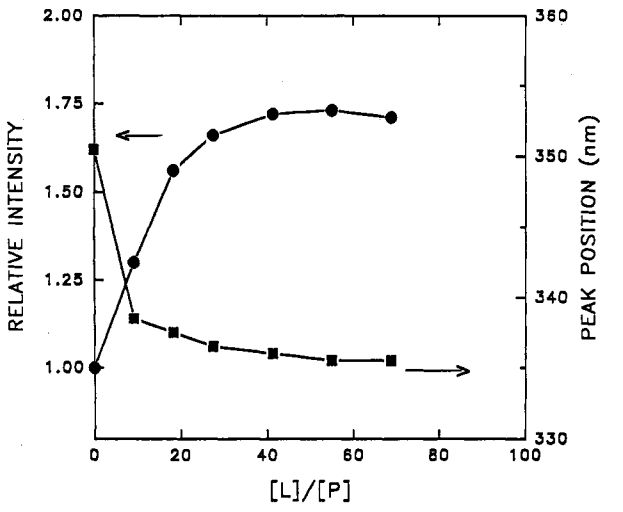

FIGURE 1: Fluorescence spectral behavior of MSH-II in the presence of POPS vesicles: [peptide] = 10^{-5} M; temperature 20 °C; excitation wavelength, 295 nm. The increase in fluorescence intensity (●) and the shift of the wavelength of maximum emission (■) are shown.

Temperature Effect on Lipid–Peptide Interaction. The data presented above were all measured under temperature conditions where the lipid systems were in the liquid-crystalline phase. A full temperature study, including temperatures below the lipid phase transition, was conducted on lipid–peptide complexes of POPS and DMPS vesicles at ratios in excess of those corresponding to the saturating ratios (determined in the liquid-crystalline phase). A direct correlation between the lipid phase transition and fluorescence intensity (Figure 2a), spectral maxima (Figure 2b), and fluorescence anisotropy (Figure 2c) of the peptides in the lipid complex was observed. Similar observations were seen in the case of DMPS vesicles. This temperature data indicated a broad temperature-induced phase transition near 36 °C for DMPS and around 10 °C for POPS. The phase transition temperatures were broader and the midpoints were not exactly the same as those observed for lipid vesicles in the absence of peptides (DMPS, pH 7, T_m = 38 °C; POPS, pH 7, T_m = 12 °C; unpublished data). This

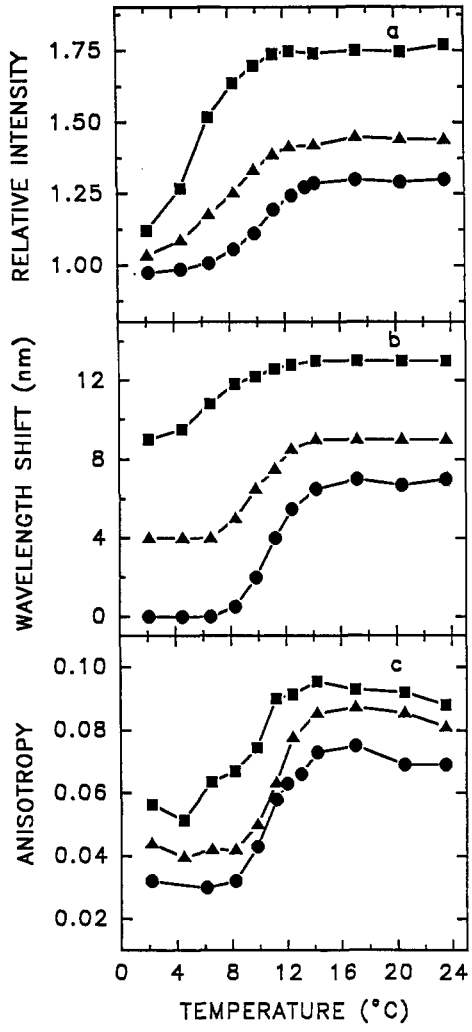

FIGURE 2: Temperature dependence of fluorescence observables for α-MSH (●), MSH-I (▲), and MSH-II (■) incorporated into POPS vesicles; L/P > plateau values. (a) Fluorescence of peptide–lipid complex relative to that of peptide in aqueous solution. (b) Spectral maximum shift to higher energy of peptide–lipid complex relative to peptide in aqueous solution. (c) Anisotropy of peptide–lipid complex. Excitation wavelength, 295 nm; [peptide] = 10^{-5} M.

may be due to the interaction of peptides with the lipid vesicles, affecting the bilayer structure.

In the interpretation of these observations, it was important to note that the fluorescence anisotropy of all of the lipid–peptide complexes, at temperatures where the vesicles exist in the gel phase, was greater than the value for the peptide free in solution. Also, in the gel phase the fluorescence spectral maxima for the MSH-I and MSH-II lipid complexes were shifted to higher energy by 4 and 9 nm, respectively, relative to that of the free peptide. The spectral maximum for the α-MSH–lipid complex in the gel phase was the same as that in aqueous solution. The addition of even greater quantities of lipid did not affect these values. The anisotropy of the α-MSH complex is higher than the solution value, indicating that this peptide was bound to the acidic lipid vesicle. Hence, all peptides were still bound to the acidic lipids under the conditions of the experiment. The temperature data suggest that the phase and structure of the lipid control the extent of interaction of the peptide with the lipid environment. In the gel phase, the tryptophan residue may become more exposed to the aqueous environment as a result of extrusion from the lipid interior by the ordering and rigidity of the vesicles (Yamashita et al., 1989). When the lipid structure becomes more fluid and less ordered, the tryptophan residue may be able to penetrate further into the lipid bilayer. Consistent with this view the data in Figure 2b could be interpreted as showing that the degree of exposure of the tryptophan residue in the gel-phase lipid–peptide complex was different for each of the three peptides. In the case of α-MSH, while the anisotropy evidence suggests that the peptide was bound to the gel-phase lipid, the tryptophan residue remained exposed to the aqueous medium. This rationalization implies that for MSH-I the tryptophan residue was partially exposed, while in MSH-II the tryptophan residue was less exposed than that in MSH-I. Above the phase transition, the spectral maxima and the fluorescence intensity changes were greatest for MSH-II, and so it may be reasonable to suggest that in the liquid-crystalline phase it was able to enter into the lipid interior.

An alternate rationalization may be that the fluorescence changes were due to changes in the microenvironment of the indole ring, owing to structural changes of the peptides on binding to the lipid vesicles. However, MSH-II is a cyclic peptide, α-MSH is a linear peptide, and Ac-α-MSH(7–10)-NH_2 is a very short tetramer, and obviously all three have different structures in solution. Yet there is a close similarity between all of the fluorescence parameters measured for these peptides in aqueous solution. Hence, this alternative view does not appear to have any support. Furthermore, it is not expected that the extent of accessibility to water would be different for such small peptides.

The temperature effect on the fluorescence anisotropy (Figure 2c) supported the rationalization that was presented. It was seen that the anisotropy in the gel-phase lipid of the peptides varied in the order MSH-II > MSH-I > α-MSH. This would appear to be consistent with the notion that the tryptophan in MSH-II is in a more restricted environment than either of the other two peptides. It follows then that in the case of α-MSH the tryptophan residue cannot penetrate into the lipid interior to the same extent as the other two peptides, even in the liquid-crystalline phase; hence its significantly lower fluorescence anisotropy in both lipid phases. A corollary of this interpretation of the data is that the binding of MSH-II to the lipid phase may be greater and its structure within the lipid vesicles may be different from that of α-MSH.

Determination of Binding Constants. The binding equilibrium of a peptide, in the case of independent binding sites, to a lipid vesicle where one molecule of peptide (P) forms a complex (PL_n) with n molecules of the lipid (L) (Surewicz & Epand, 1984; Jain et al., 1985) may be described by the conventional binding isotherm:

$$X = [P_f]/(K_d + n[P_f]) \quad (1)$$

where $X = [P_b]/[L_T]$ is the number of moles of peptide bound (P_b) per mole of total lipid (L_T). $[P_f]$ is the concentration of free peptide, and K_d is the dissociation constant.

From fluorescence measurements, using titration data such as that illustrated in Figure 3, the values of $[P_b]$ and the parameter X may be determined. This figure describes the variation in fluorescence intensity of α-MSH, MSH-I, and MSH-II after the addition of POPS (Figure 3a) and DMPS (Figure 3b) vesicles.

The values of n and K_d may be determined empirically from the conventional reciprocal plot or, alternately, from a Scatchard plot analysis using the following equation:

$$X/[P_f] = 1/K_d - nX/K_d \quad (2)$$

The Scatchard plot of the data for the binding of MSH-I to POPS vesicles using this conventional isotherm is shown in Figure 4a. Such a plot was typical of the data for the interactions of the different hormones with the lipid systems

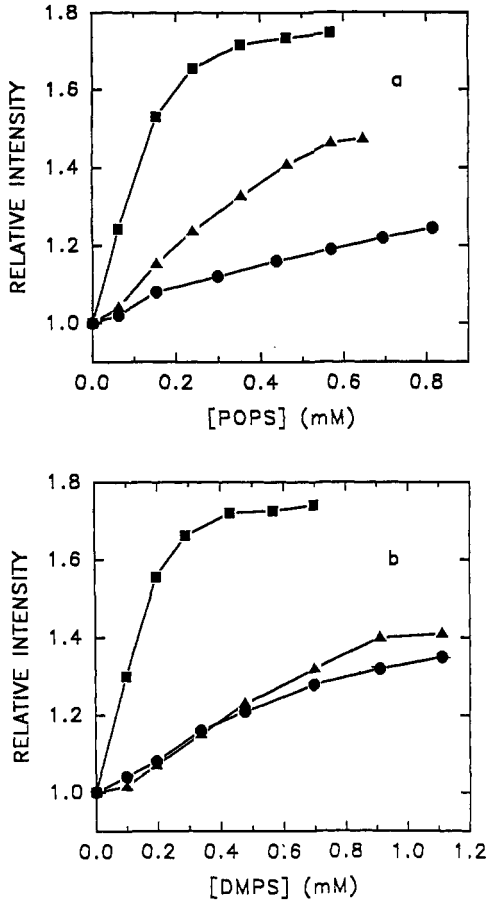

FIGURE 3: Relative increase in fluorescence intensity at 340 nm of α-MSH (●), MSH-I (▲), and MSH-II (■) on addition of acidic lipid vesicles: (a) POPS vesicles, 20 °C; (b) DMPS vesicles, 40 °C. [peptide] = 10^{-5} M.

studied. However, in several cases the point at the lowest ratio of $[L_T]/[P_T]$ significantly deviated from linearity with the remaining points. This was considered to be due to the fact that the number of lipid molecules was considerably less than n, with a different stoichiometry or a significant neutralization of the charge distribution of the negatively charged acidic vesicle surface by the high local concentration of peptide. The values of K_d and n from the conventional Scatchard plots and the binding free energies for each system are listed in Table IV.

The lack of any evidence of binding of the peptide to neutral lipids suggests that the electrostatic effect of binding of hormone to the vesicles should be considered for these systems, as described by Seelig and MacDonald (1989). The negatively charged vesicle surface attracts the positively charged peptide to the vicinity of the vesicle, increasing the concentration of free peptide near the lipid–water interface. The surface charge will facilitate the incorporation of the peptide into the lipid matrix, altering the surface charge density, which in turn affects the attraction of the hormone to the aqueous diffuse layer. Further, as the amount of incorporated peptide increases, additional peptide insertion would be diminished. When the electrostatic effect is neglected, as it was in the above treatment with the conventional form of the Scatchard plot, then only apparent values of the binding parameters would be obtained. The electrostatic effect on the binding of small peptides such as neuropeptide substance P (Seelig & MacDonald, 1989) and melittin (Beschiaschvili & Seelig, 1990; Kuchinka & Seelig, 1989) to acidic lipids has been determined using procedures based on Gouy–Chapman theory (McLaughlin, 1977) and was well described in these reports.

The partial neutralization of negatively charged lipids by the incorporation of positively charged peptides results in a decrease in the Gouy–Chapman potential. The surface charge density (S) at the surface of the vesicle is given by the relationship (McLaughlin, 1977):

$$S = e_o(z_L X_L + z_P X_b)/\{A_L(1 + X_b A_P/A_L)\} \quad (3)$$

where e_o is the elementary charge, X_L is the mole fraction of charged lipids (of charge z_L), z_P is the charge of the peptide, A_L and A_P are the surface areas of lipid and peptide, respectively, and X_b is $X/0.56$. This value of X_b accounts for the concept that only the outer membrane surface is involved in the electrostatic attraction, and the factor of 0.56 is derived from the fractional concentration of lipids in the outer surface of vesicles with a 100-nm diameter (Beschiaschvili & Seelig, 1990; Cullis & Hope, 1985). The value of A_L was assumed to be 60 Å^2 (Cullis & Hope, 1985). Values between 150 and 250 Å^2 for A_P for peptides in vesicles and bilayers have been proposed (Seelig & MacDonald, 1989; Beschiaschvili & Seelig, 1990), and an approximate value of 200 Å^2 was used in this work (the choice of a value of A_P between 150 and 250 Å^2 did not significantly affect the value of S when X was small, as in the present case). The net charge of lipids and peptides was −1 and +1, respectively.

The variation in the surface charge density S generates a Gouy–Chapman potential, which is described by the relationship (McLaughlin, 1977):

$$S = \{(2000 e_R e_o RT \sum c_i[\exp(-z_i F_o - \psi_o/RT - 1)]\}^{1/2} \quad (4)$$

where e_R is the dielectric constant of water, e_o is the permittivity of free space, R is the gas constant, F_o is the Faraday constant, c_i is the concentration of the ith electrolyte in the bulk aqueous phase (in moles/liter), and z_i is the signed charge of the ith species. The Gouy–Chapman potential, ψ_o, influences the distribution of charged molecules in the medium by imposing two populations related, in equilibrium, through the Boltzmann equation:

$$[P_M] = [P_{eq}] \exp(-\psi_o z_P F_o/RT) \quad (5)$$

where $[P_M]$ is the concentration of charged peptides adjacent to the membrane surface and $[P_{eq}]$ or $[P_f]$ is the concentration in the bulk solution.

Considering the electrostatic interaction, one has to use the value of $[P_M]$ instead of $[P_f]$ (concentration of peptide in the bulk solution) both in eq 1 for the binding isotherm and in eq 2 for the Scatchard plot. This means that the association constant is determined for the interaction between lipids in the bilayer and peptides accumulated near the surface due to the electrostatic effect. The Scatchard plots of $X_b/[P_M]$ versus X_b, of which Figure 4b (MSH-I in POPS vesicles) is an example, were not significantly different in shape from the conventional Scatchard plots where the effect of electrostatic potential was not considered. The numerical value of the K_d was similar to that obtained from the conventional plots but differed by 3 orders of magnitude (Table IV). The value of n, the number of lipid molecules associated with the peptide in the complex, was about one-half that found from the conventional plots. The result of the application of the Gouy–Chapman electrostatic potential to the experimental data differs from that reported for the interaction of other small peptides with acidic lipids, including neuropeptide P (Seelig & MacDonald, 1989) and melittin (Beschiaschvili & Seelig, 1990). In these latter cases, application of the Gouy–Chapman potential to the titration data resulted in Scatchard plots with slopes of zero and the implication that the binding of the peptide to the lipid was in the form of a partition function.

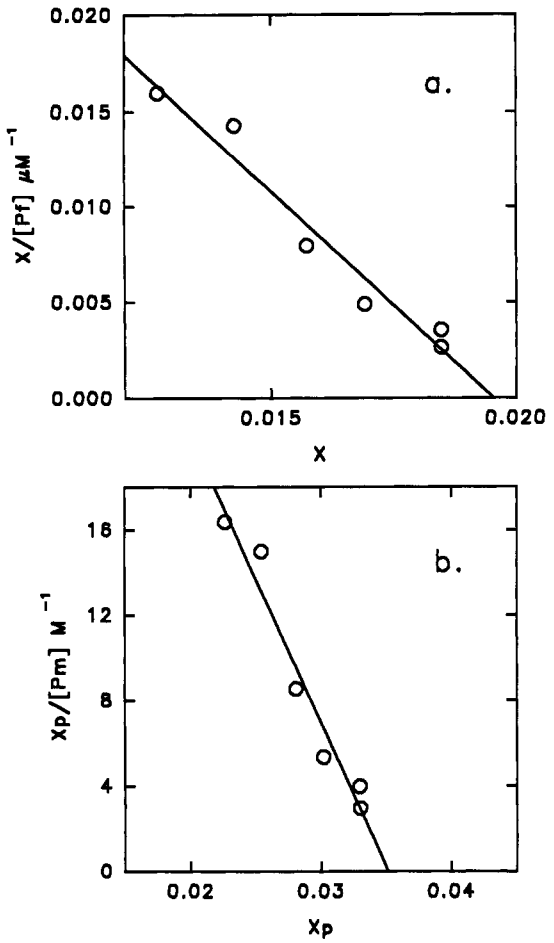

FIGURE 4: Scatchard plot analysis of the titration of fluorescence increase of MSH-I with POPS vesicles, 20 °C: (a) conventional analysis; (b) analysis with Gouy–Chapman correction for the electrostatic potential of the lipid vesicle surface. The solid line represents the best linear regression fit to the data.

Table IV: Binding Parameters of Melanotropin Peptides to Lipids from Scatchard Plot Analyses

	POPS Vesicles[a]		
	α-MSH	MSH-I	MSH-II
no correction			
n	46	51	19
K_d (μM)	95	22	8.9
$-\Delta G$ (kcal/M)	5.5	6.3	6.9
Gouy–Chapman corrected			
n	25	29	10
K_d (mM)	96	20	7.8
$-\Delta G$ (kcal/M)	1.4	2.3	2.9

	DMPS Vesicles[a]			
	α-MSH	MSH-I	MSH-II	MSH(7–10)
no correction				
n	39	46	20	64
K_d (μM)	147	28	15	58
$-\Delta G$ (kcal/M)	5.5	6.6	6.9	6.1
Gouy–Chapman corrected				
n	20	25	10	36
K_d (mM)	153	26	15	59
$-\Delta G$ (kcal/M)	1.2	2.3	2.7	1.8

	MML Micelles[a]		
	α-MSH	MSH-I	MSH(7–10)
n	20	14	23
K_d (μM)	189	278	200
$-\Delta G$ (kcal/M)	5.1	4.8	5.0

[a] The temperature for the different lipid systems were as follows: POPS, 20 °C; DMPS, 40 °C; MML, 20 °C.

In the present work, the interaction of the MSH peptides with acidic lipids retains binding according to an equilibrium relationship that depends on the concentration of both the lipid and the peptide. One possible reason for this may be that the MSH peptides were not as highly charged as neuropeptide P (+3) or melittin (+6).

The accumulation of peptides at the surface of the vesicles will likely affect the surface pH, changing it from the bulk pH. This may result in a change in the net charge of the peptides as the histidine residue becomes protonated. A pH study on the fluorescence behavior of the peptides showed a decrease in intensity of 15% between pH 7 and 3. Between these pH values, the histidine residue can become protonated, increasing the peptide net charge to +2. At pH <3 there is a significant amount of fluorescence quenching, probably due to the protonation of the glutamic acid residue. However, for all peptides, upon interaction with the vesicles, there was a significant increase in fluorescence, and hence the pH could not have been dramatically different from that of the bulk solution. Furthermore, in the calculations of the Gouy–Chapman potentials, when the net charge of the peptide was changed to +2, there were only minor changes in K_d and n.

The important information obtained from the binding parameters in this work was the comparative affinities of the different peptides for the acidic lipid systems studied. The relative association of the peptides for the lipid vesicles is MSH-II > MSH-I > α-MSH. This is consistent with the fluorescence intensity and fluorescence anisotropy results, where MSH-II has the greatest relative increase in fluorescence intensity and the highest anisotropy values. It is suggested that such observations would be obtained if MSH-II were more tightly bound to the lipid vesicle system, because its smaller size and more compact structure may allow a deeper penetration into the lipid environment.

The number of lipids associated with peptide in the complex is significantly less for MSH-II as well. The results for the binding of MSH(7–10) to DMPS vesicles indicate that its association was significantly less than either MSH-I or MSH-II. This may either be because of its very small size or because it is unable to adopt the favorable peptide conformation that exists in MSH-I and MSH-II. It has been shown in a recent NMR study (Sugg et al., 1986) that MSH-I adopts a predominant backbone conformation that is a non-hydrogen-bonded β-structure. Further, MSH-II is a cyclic lactam analog in which this latter β-structure is locked into place, owing to the lactam formed between Asp^5 and Lys^{10} in the α-MSH-(4–10) shortened peptide.

The larger values of the dissociation constants of the peptides in DMPS vesicles compared to POPS vesicles are likely due to the higher temperatures of the experiments with DMPS. The binding data of the peptides with MML show that the interaction with micelles is nonspecific and may reflect the hydrophobic association of the micelles and peptides.

There appears to be a strong correlation between the biological activity of the peptides and the binding parameters measured herein. MSH-II is 90 times more potent and MSH-I is 5 times more potent in a lizard skin assay than α-MSH, and both have a significantly prolonged activity. This correlation suggests that the extent of interaction of the peptide with the lipid environment of the cell plays a large role in receptor-mediated response. This is consistent with Schwyzer's concept that the peptide first interacts with the membrane surface through electrostatic attraction and then is subsequently incorporated near the receptor, where its message segment transmits the observed biological response (Sargent & Schwyzer, 1986).

Table V: Fluorescence Decay Parameters of Melanotropin Peptides[a] Determined from Global Analysis[b]

temp (°C)	τ_1	τ_2	τ_3	α_1	α_2	α_3
α-MSH						
20	3.22	1.49	0.33	0.47	0.35	0.18
30	2.58	1.37	0.35	0.48	0.31	0.21
40	2.13	1.29	0.33	0.36	0.43	0.21
MSH(7–10)						
20	2.32	1.11	0.12	0.55	0.30	0.15
30	2.04	1.40	0.31	0.32	0.52	0.16
40	2.08	1.24	0.26	0.36	0.52	0.12
MSH-I						
20	3.21	1.36	0.23	0.45	0.37	0.18
30	2.76	1.50	0.35	0.38	0.41	0.21
40	2.20	1.27	0.30	0.33	0.47	0.20
MSH-II						
20	3.94	1.73	0.40	0.27	0.46	0.27
30	3.30	1.58	0.42	0.25	0.48	0.28
40	2.75	1.35	0.38	0.21	0.53	0.26

[a] The [peptide] = 10^{-5} M; 0.01 M phosphate buffer, pH 7.0. Excitation wavelength was 295 nm. [b] τ_i are the decay times in nanoseconds of each fluorescence decay component, determined from a global analysis of the several data sets measured across the fluorescence spectrum; α_i are the normalized concentrations obtained from an integration of the DAS. The standard errors in the values of τ_1 and τ_2 were $<\pm 0.01$, for τ_3 $<\pm 0.005$, and for the preexponential terms $<\pm 0.01$.

Time-Resolved Fluorescence in Aqueous Solution. Time-resolved fluorescence measurements showed that the decay of the tryptophan fluorescence in the melanotropin peptides was best described by multiexponential decay kinetics. In every case, three exponential decay components were required to fit the experimental decay data, as judged by a number of statistical parameters (MacKinnon et al., 1975). This fluorescence decay behavior of tryptophan in the melanotropins was similar to that found for other small peptides containing a single tryptophan residue in aqueous solution (Cavatorta et al., 1991; Willis & Szabo, 1992). The multiexponential decay has been rationalized as originating from the fluorescence of different rotational conformers of the indole ring around the C_α–C_β bond of the alanyl side chain (Willis & Szabo, 1992; Ross et al., 1992).

The fluorescence decay parameters of each of the melanotropin peptides in aqueous buffer (pH 7) at 20, 30, and 40 °C are listed in Table V. At 20 °C, the longest decay time ranged in value from 3.21 to 3.94 ns for each of the peptides. An intermediate decay time with values between 1.37 and 1.58 ns and a short decay time with values between 0.117 and 0.400 ns were also observed. The short decay time component was not due to an impurity nor to any scattering artifact. As seen from Table V, it represented a significant proportion of the three decay components. These decay time values are typical of those found for small peptides in aqueous buffer. An exception was the fluorescence decay of the short-fragment analog, MSH(7–10), which exhibited significantly shorter decay times. For each of the peptides, the long decay time component decreased markedly with increasing temperature, behavior which is commonly observed for tryptophan in peptides and proteins. The other two decay times did not change very much with temperature. At the present time, a satisfactory rationalization of this differing temperature behavior has not been advanced, nor is it fully understood why the different rotamers have significantly different decay time values. Perhaps the orientation or position of the indole ring of the tryptophan causes it to interact differently with the peptide backbone of the protein or peptide, and the proximity to, or alignment with, the amide carbonyl dipole is responsible for modifying the lifetime of the excited singlet state of a particular rotamer.

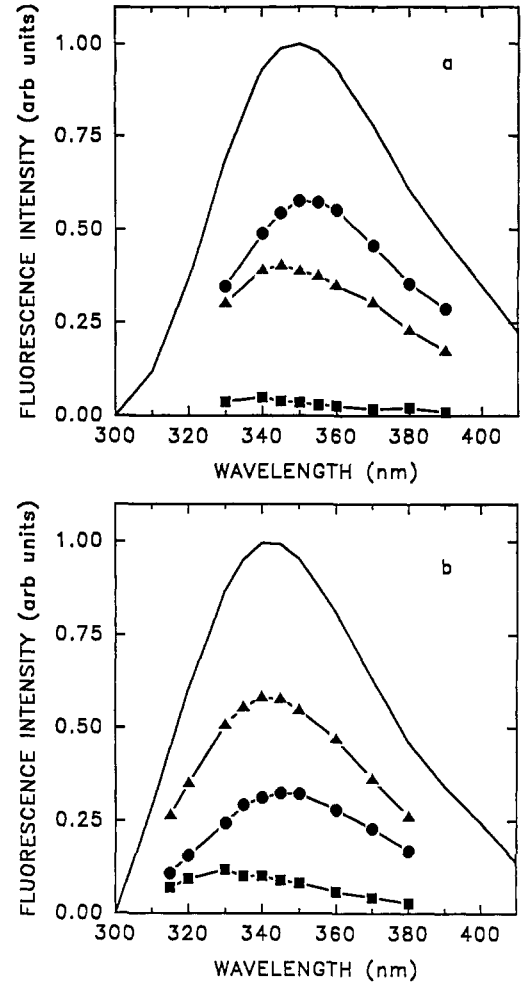

FIGURE 5: DAS of MSH-I at 20 °C: (a) in aqueous solution, pH 7, 3.21-ns component (●), 1.36-ns component (▲), 0.23-ns component (■), and steady-state spectrum (—); (b) in POPS complex, L/P = 75, 5.25-ns component (●), 1.93-ns component (▲), 0.38-ns component (■), and steady-state spectrum (—)

For a given peptide, the decay times were nearly constant across the fluorescence spectrum. This permits a global analysis of the data sets measured at different wavelengths to obtain the fluorescence spectrum of each decay component. The decay-associated spectra (DAS) (Knutson et al., 1983) were generated for each peptide under the different conditions of the experiments in this study. A typical DAS is shown in Figure 5a, which is that for MSH-I at 20 °C. The DAS for MSH-I at 40 °C is shown in Figure 6a. At 20 °C, the long decay time component had more than twice the intensity of the intermediate decay time component. At 40 °C these two components had nearly equal intensities. At both temperatures, the shortest decay component made only a small contribution to the total fluorescence intensity. At 20 °C, the spectral maximum of each component was the same as the steady-state maximum, while at 40 °C it appeared as if the spectral maximum of the intermediate decay time had shifted ca. 5 nm to higher energy. For α-MSH, MSH-I, and MSH-(7–10) at 20 °C, the relative fluorescence contributions of the three components were in the following ranges: 72–78, 21–25, and 1–3. In the case of MSH-II at 20 °C the ratio was notably different: 54:40:6.

The integrated area of each DAS component is proportional to the relative concentration of each component conformer (Willis & Szabo, 1992). For α-MSH, and MSH-I, the relative populations were 45–47, 35–37, and 18, for the long, intermediate, and short decay time components, respectively.

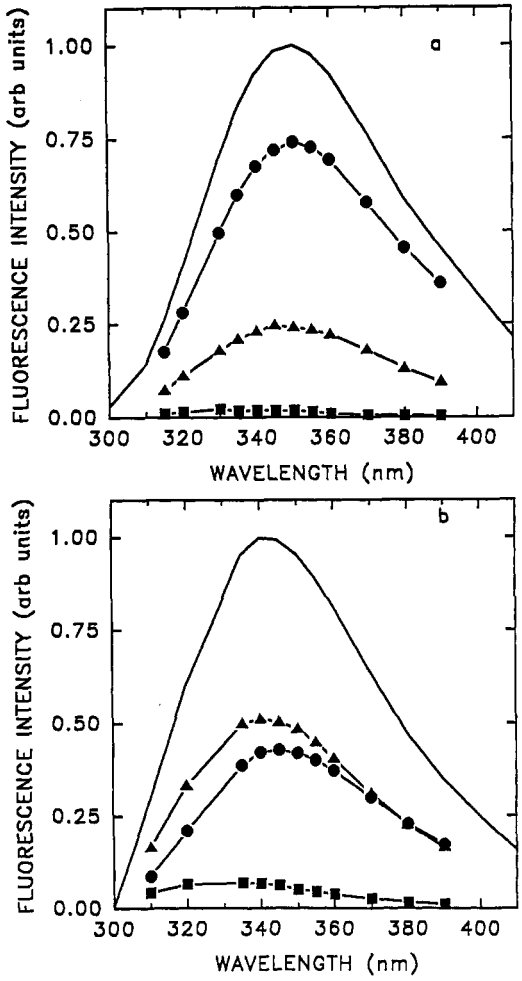

FIGURE 6: DAS of MSH-I, 40 °C: (a) in aqueous solution, pH 7, 2.20-ns component (●), 1.27-ns component (▲), 0.30-ns component (■), and steady-state spectrum (—); (b) in DMPS complex, L/P = 100, 4.53-ns component (●), 1.70-ns component (▲), 0.42-ns component (■), and steady-state spectrum (—)

The relative proportions of the decay components for both MSH(7–10) and MSH-II were different from those of α-MSH and MSH-I and different from each other. For MSH(7–10) the relative proportions were 55, 30, and 15. In the case of MSH-II, the corresponding values were markedly different from those of any of the other peptides, since the intermediate decay time component was present in the greatest proportion, the proportions being 27, 46, and 27 (Table V). This difference in the case of MSH-II must signify that it exists in a conformation significantly different from those of the other peptides. The other peptides have a totally random structure in solution, the only difference between α-MSH and MSH-I being that the latter peptide has Nle substituted for the Met[4] and D-Phe for the L-Phe[7] in α-MSH. Indeed, the fluorescence decay behavior for these two peptides was very similar except at 30 °C. MSH(7–10) is a tetrapeptide and obviously would have a solution structure different from the other two tetradecapeptides. MSH-II, on the other hand, is a cyclic lactam and so has a different structure in solution. Because of the lactam structure, its peptide backbone would be restricted and it would be unable to undergo any significant temperature-induced structural change. It is noteworthy that the tryptophan rotamer distribution in PTH and PTH-related peptides (Willis & Szabo, 1992), when in a random structure, had nearly the same proportions (PTH 1–34, 6 M GuHCl; 48, 38, and 14) of the decay components as α-MSH and MSH-I. At the higher temperature of 40 °C, the intermediate decay time component was the most populous, indicating a change

Table VI: Fluorescence Decay Parameters of Melanotropin Peptides in the Presence of Lipids,[a] Determined from Global Analysis[b]

lipid (temp, °C)	τ_1	τ_2	τ_3	α_1	α_2	α_3
α-MSH						
MML (20)	5.10	2.09	0.43	0.33	0.44	0.23
POPS (20)	4.56	2.16	0.55	0.29	0.48	0.23
DMPG (30)	4.13	1.81	0.46	0.16	0.49	0.35
DMPS (40)	3.75	1.55	0.37	0.14	0.55	0.30
MSH(7–10)						
MML (20)	4.58	1.86	0.38	0.27	0.49	0.24
DMPG (30)	3.64	1.54	0.43	0.14	0.53	0.33
DMPS (40)	3.83	1.46	0.36	0.16	0.38	0.27
MSH-I						
MML (20)	5.19	1.93	0.38	0.31	0.42	0.27
POPS (20)	5.25	2.28	0.53	0.18	0.52	0.29
DMPG (30)	4.77	1.93	0.49	0.14	0.47	0.39
DMPS (40)	4.53	1.70	0.42	0.10	0.52	0.37
MSH-II						
POPS (20)	5.66	2.43	0.54	0.14	0.48	0.37
DMPG (30)	4.88	1.74	0.41	0.08	0.46	0.45
DMPS (40)	4.76	1.83	0.43	0.14	0.44	0.42

[a] The [peptide] was either 1 or 2×10^{-5} M; 0.01 M phosphate buffer, pH 7.0. The L/P ratio was >saturation value. Excitation wavelength was 295 nm. [b] τ_i are the decay times in nanoseconds of each fluorescence decay component, determined from a global analysis of several data sets measured across the fluorescence spectrum; α_i are the normalized concentrations obtained from an integration of the DAS. The standard errors in the values of τ_1 and τ_2 were $<\pm 0.01$, for τ_3 $<\pm 0.005$, and for the preexponential terms $<\pm 0.01$.

in the rotamer distribution with temperature which may be related to changes in the peptide structural distribution. In the case of MSH-II, the intermediate decay time component was the most important component at all temperatures, increasing from 46% to 53% from 20 to 40 °C. This was accompanied by a decrease in the proportion of the long decay time component. In the case of every peptide, there was hardly any change in the relative proportion of the short decay time component.

Time-Resolved Fluorescence in Peptide–Lipid Complexes. The time-resolved fluorescence parameters for the peptides in lipid complexes are summarized in Table VI. The data for these experiments were conducted at lipid/peptide ratios corresponding to the plateau values of the steady-state fluorescence. The temperatures for the vesicle complexes were those where the vesicles were in the liquid-crystalline state for each lipid type. In every case, the two longer decay times of the peptide increased in the lipid environment. This behavior would be consistent with the indole ring of the tryptophan residue being located in the lipid bilayer, reducing collisional nonradiative deactivation processes with solvent molecules. The long decay time of MSH-II in POPS vesicles is the longest of the corresponding decay times of any of the peptides. This fact, taken together with the steady-state data and binding analysis, suggests that MSH-II, the most potent biologically active peptide, is the one which penetrates most into the lipid matrix.

The DAS of the MSH-I–POPS complex (20 °C) and the MSH-I–DMPS complex (40 °C) are shown in Figures 5 and 6, respectively. Compared to the DAS in solution at the same temperatures, it is immediately evident that the relative proportions of the different decay time components change when the peptide is in a lipid vesicle complex. Examination of the relative proportions of each decay component (Table VI) reveals information on the structural changes that occur when the peptides interact with the lipids. In the case of MSH-II, the proportion of the long decay time component decreases, while that of the shortest decay time component increases in each of the lipid complexes. Furthermore, the relative proportions are similar for each MSH-II complex. It

is significant that MSH-I in DMPG and DMPS has the same relative proportions of the decay components as MSH-II. This implies that MSH-I assumes a structure similar to that of MSH-II in the lipid vesicles. Since the latter is constrained to a reversed turn structure because of the lactam bridge between Asp^5 and Lys^{10}, the data suggest that MSH-I forms the same turn structure in the presence of acidic lipids. NMR evidence (Sugg et al., 1986) and molecular dynamics simulations (Al-Obeidi et al., 1989) both indicate that the conserved His^6-Phe^7-Arg^8-Trp^9 sequence prefers to exist in a β-turn conformation. When the phenylalanine is in the D configuration, such a reverse turn structure results in the lipophilic and hydrophilic side chains being on opposite faces of the peptide. Furthermore, the presence of the D-amino acid tends to make the structure more compact in its vicinity. The fluorescence results on MSH-I in lipids are fully consistent with that peptide adopting a predominant turn configuration similar to the structurally restricted MSH-II. In the case of α-MSH, it appears that this peptide cannot adopt this configuration until it associates with the acidic lipid DMPS at 40 °C, since only under these conditions do the relative proportions of the decay components become similar to those of MSH-II. At the lower temperature of 20 °C in POPS vesicles, the peptide structure is different from that in aqueous solution, but does not adopt a reversed turn structure.

Finally, in the MML micelles the relative proportions of the three decay time components were similar to those determined in aqueous solution, except in this case it is the intermediate decay time component that is present in the greatest amount. This indicates that, in the micelles, the β-turn structure is not adopted by the peptides.

SUMMARY AND CONCLUSIONS

The combination of the steady-state fluorescence data, the time-resolved fluorescence parameters, and the lipid binding behavior of the melanotropin peptides shows that the peptides adopt significantly different structures in acidic vesicles from those in aqueous solution. The properties in the lipid complexes are strongly correlated with the relative biological activity of the peptides. Thus, the data suggest that the tryptophan of MSH-II, the most potent melanotropin peptide with a restricted β-turn type lactam structure, may penetrate farthest into the lipid matrix. MSH-I adopts a similar turn structure upon interaction with the acidic lipids, but the degree of incorporation of its tryptophan residue is less than that of MSH-II. The least active peptide, α-MSH, has the lowest vesicle affinity of the three peptides, and it is suggested that it is less able to adopt the active β-turn structure upon interaction with the lipids. The tryptophan penetration into the lipid environment is also less. There appears to be a correlation between the apparent degree of penetration of the tryptophan residue, the affinity constants of the peptides for the acidic vesicles, and the ability to form a turn structure in the vicinity of the tryptophan residue and the biological activity of the peptides.

REFERENCES

Al-Obeidi, F., Hadley, M. E., Pettitt, B. M., & Hruby, V. J. (1989a) *J. Am. Chem. Soc. 111*, 3413–3416.

Al-Obeidi, F., Castrucci, A. M. L., Hadley, M. E., & Hruby, V. J. (1989b) *J. Med. Chem. 32*, 2555–2561.

Beechem, J. M., & Brand, L. (1985) *Annu. Rev. Biochem. 54*, 43–71.

Beschiaschvili, G., & Seelig, J. (1990) *Biochemistry 29*, 52–58.

Castrucci, A. M. L., Sawyer, T. K., Al-Obeidi, F., Hruby, V. J., & Hadley, M. E. (1990) *Drugs Future 15*, 41–55.

Cavatorta, P., Spisni, A., Szabo, A. G., Farruggia, G., Franzoni, L., & Masotti, L. (1989) *Biopolymers 28*, 441–463.

Cavatorta, P., Sartor, G., Neyroz, P., Farruggia, G., Franzoni, L., Szabo, A. G., & Spisni, A. (1991) *Biopolymers 31*, 653–661.

Chung, L. A., Lear, J. D., & DeGrado, W. F. (1992) *Biochemistry 31*, 6608–6616.

Cullis, P. R., & Hope, M. J. (1985) *Biochemistry of Lipids and Membranes* (Vance, D. E., & Vance, J. E., Eeds.) pp 25–72, Benjamin/Cummings, Menlo Park, CA.

Donzel, B., Gauduchon, P., & Wahl, P. (1974) *J. Am. Chem. Soc. 96*, 801–808.

Hadley, M. E., & Castrucci, A. M. L. (1988) *The Melanotropic Peptides* (Hadley, M. E., Ed.) Vol. III, pp 15–25, CRC Press, Boca Raton, FL.

Hadley, M. E., Abdel-Malek, Z. A., Marwan, M. M., Kreutzfeld, K. L., & Hruby, V. J. (1985) *Endocrinol. Res. 11*, 157–170.

Hope, M. J., Bally, M. B., Webb, G., & Cullis, P. R. (1985) *Biochim. Biophys. Acta 812*, 55–65

Hruby, V. J., Wilkes, B. C., Cody, W. L., Sawyer, T. K., & Hadley, M. E. (1984) *Peptide and Protein Reviews* (Hearn, M. T. W., Ed.) Vol. 3, pp 1–64, Marcel Dekker, Inc., New York.

Hruby, V. J., Wilkes, B. C., Hadley, M. E., Al-Obeidi, F., Sawyer, T. K., Staples, D. J., deVaux, A. E., Dym, D., Castrucci, A. M. L., Hintz, M. F., Riehm, J. P., & Rao, K. R. (1987) *J. Med. Chem. 30*, 2126–2130.

Hutnik, C. M., & Szabo, A. G. (1989) *Biochemistry, 28*, 3923–3934.

Jain, M. K., Rogers, J., Simpson, L., & Gierasch, L. M. (1985) *Biochim. Biophys. Acta 846*, 153–162.

Knutson, J. R., Beechem, J. M., & Brand, L. (1983) *Chem. Phys. Lett. 102*, 501–507.

Kuchinka, E., & Seelig, J. (1989) *Biochemistry 28*, 4216–4221.

MacKinnon, A. E., Szabo, A. G., & Miller, D. R. (1977) *J. Phys. Chem. 81*, 1564–1570

McKnight, C. J., Rafalski, M., & Geirasch, L. M. (1991) *Biochemistry 30*, 6214–6246.

McLaughlin, S. (1977) *Curr. Top. Membr. Transp. 9*, 71–144.

Ross, J. B. A., Wyssbrod, H. R., Porter, R. A., Schwartz, G. P., Michaels, C. A., & Laws, W. R. (1992) *Biochemistry 31*, 1585–1594.

Sargent, D. F., & Schwyzer, R. (1986) *Proc. Natl. Acad. Sci. U.S.A. 83*, 5774–5778.

Sawyer, T. K., Sanfilippo, P. J., Hruby, V. J., Engel, M. H., Heward, C. B., Burnett, K. B., & Hadley, M. E. (1980) *Proc. Natl. Acad. Sci. U.S.A. 77*, 5754-5758.

Sawyer, T. K., Hadley, M. E., Wilkes, B. C., & Hruby, V. J. (1988) *The Melanotropic Peptides* (Hadley, M. E., Ed.) Vol. III, pp 59–74, CRC Press, Boca Raton FL.

Schwyzer, R. (1986) *Biochemistry 25*, 6335–6341.

Seelig, A., & MacDonald, P. M. (1989) *Biochemistry 28*, 2490–2496.

Seelig, A., Allegrini, P. R., & Seelig, J., (1988) *Biochim. Biophys. Acta 939*, 267–276.

Sugg, E. E., Cody, W. L., Abdel-Malek, Z., Hadley, M. E., & Hruby, V. J. (1986) *Biopolymers 25*, 2029–2042.

Surewicz, W. K., & Epand, R. M. (1984) *Biochemistry 23*, 6072–6077.

Szabo, A. G., & Rayner, D. M. (1980) *J. Am. Chem. Soc. 102*, 554–563.

Willis, K. J., & Szabo, A. G. (1989) *Biochemistry 28*, 4902–4908.

Willis, K. J., & Szabo, A. G. (1992) *Biochemistry 31*, 8924–8931.

Yamashita, S., Szabo, A. G., Krajcarski, D. T., & Yamasaki, N. (1989) *Bull. Chem. Soc. Jpn. 62*, 3075–3080.